

LSO/LYSO Crystals for Future HEP Experiments

This article has been downloaded from IOPscience. Please scroll down to see the full text article.

2011 J. Phys.: Conf. Ser. 293 012004

(<http://iopscience.iop.org/1742-6596/293/1/012004>)

View [the table of contents for this issue](#), or go to the [journal homepage](#) for more

Download details:

IP Address: 131.215.220.186

The article was downloaded on 07/10/2011 at 16:28

Please note that [terms and conditions apply](#).

LSO/LYSO Crystals for Future HEP Experiments

Rihua Mao, Liyuan Zhang and Ren-Yuan Zhu

256-48, HEP, Caltech, Pasadena, CA 91125, USA

E-mail: zhu@hep.caltech.edu

Abstract. Because of their high stopping power ($X_0 = 1.14$ cm), fast ($t = 40$ ns) and bright (4 times of BGO) scintillation and good radiation hardness, cerium doped silicate based heavy crystal scintillators (LSO and LYSO) have attracted a broad interest in the high energy physics community pursuing precision electromagnetic calorimeter in severe radiation environment. We present in this paper current status of large size LSO and LYSO crystals adequate for HEP applications. The optical and scintillation properties and their radiation hardness are discussed.

1. Introduction

In the last two decades, cerium doped silicate based heavy crystal scintillators have been developed for the medical industry. As of today, mass production capabilities of lutetium oxyorthosilicate ($\text{Lu}_2(\text{SiO}_4)\text{O}$, LSO) [1] and lutetium-yttrium oxyorthosilicate ($\text{Lu}_{2(1-x)}\text{Y}_{2x}\text{SiO}_5$, LYSO) [2, 3] are established. Because of their high stopping power (> 7 g/cm³), high light yield (200 times of PWO) and fast decay time (40 ns) this material has also attracted a broad interest in the physics community pursuing precision electromagnetic calorimeter, such as the proposed SuperB forward endcap calorimeter [4], the KLOE experiment [5] and the Mu2e experiment [6]. Our initial investigation on large size ($2.5 \times 2.5 \times 20$ cm) LSO/LYSO crystals also shows that this new generation of heavy crystal scintillators has a superb radiation hardness against γ -rays [7], neutrons [8] and charged hadrons [9]. They are thus an excellent material to be used in a severe radiation environment, such as the proposed high luminosity large hadron collider (HL-LHC). The main obstacles of using these crystals in the experimental physics are two fold: the availability of high quality crystals in sufficiently large size and the high cost associated with their high melting point ($\sim 2,000^\circ$). This report is a part of an on-going R&D program to further develop this material to be of practical use at the HL-LHC.

2. Properties of Scintillating Crystals

Table 1 lists basic properties of heavy crystal scintillators: NaI(Tl), CsI(Tl), BaF₂, CeF₃, bismuth germanate ($\text{Bi}_4\text{Ge}_3\text{O}_{12}$ or BGO), lead tungstate (PbWO_4 or PWO) and LSO [10]. As shown in the table, all crystals, except CeF₃, have either been used in, or actively pursued for, high energy and nuclear physics experiments. Figure 1 is a photo showing twelve crystal samples. In addition to samples listed in Table 1 pure CsI, CsI(Na), LYSO as well as LaCl₃ and LaBr₃ are also shown in this photo although the last two are not yet in mass production stage. Samples are arranged in an order of their density, or radiation length. All non-hygroscopic samples are wrapped with white Tyvek paper as reflector. Hygroscopic NaI, CsI, LaBr₃ and LaCl₃ are sealed in packages with two ends made of quartz plates of 3 or 5 mm thick to avoid

Table 1. Properties of Heavy Crystal Scintillators with Mass Production Capability

Crystal	NaI(Tl)	CsI(Tl)	BaF ₂	CeF ₃	BGO	PbWO ₄	LSO(Ce)
Density (g/cm ³)	3.67	4.51	4.89	6.16	7.13	8.3	7.40
Melting Point (°C)	651	621	1280	1460	1050	1123	2050
Radiation Length (cm)	2.59	1.86	2.03	1.70	1.12	0.89	1.14
Molière Radius (cm)	4.13	3.57	3.10	2.41	2.23	2.00	2.07
Interaction Length (cm)	42.9	39.3	30.7	23.2	22.7	20.7	20.9
Refractive Index ^a	1.85	1.79	1.50	1.62	2.15	2.20	1.82
Hygroscopicity	Yes	Slight	No	No	No	No	No
Luminescence ^b (nm)	410	560	300	340	480	425	420
(at Peak)			220	300		420	
Decay Time ^b (ns)	245	1220	650	30	300	30	40
			0.9			10	
Light Yield ^{b,c}	100	165	36	7.3	21	0.30	85
			4.1			0.077	
d(LY)/dT ^{b,d} (%/°C)	-0.2	0.4	-1.9	~0	-0.9	-2.5	-0.2
			0.1				
Experiment	Crystal Ball	CLEO BaBar BELLE BES III	TAPS	-	L3 BELLE	CMS ALICE PrimEx Panda	SuperB KLOE

a At the wavelength of the emission maximum.

b Top line: slow component, bottom line: fast component.

c Relative light yield of samples of $1.5 X_0$ and with the PMT quantum efficiency taken out.

d At room temperature.

surface degradation. To minimize the uncertainties caused by the sample size dependence in the light output measurement all samples have a cubic shape of $1.5 \times 1.5 \times 1.5 X_0^3$, except NaI(Tl)

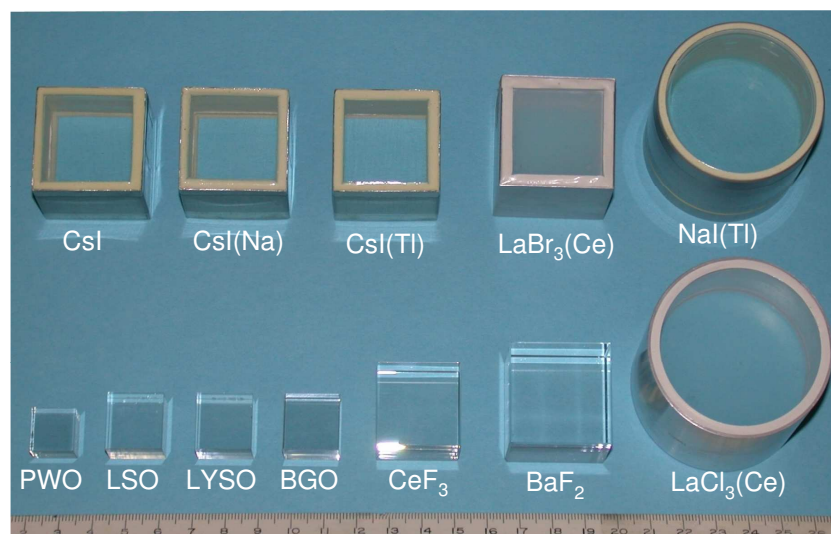


Figure 1. A photo shows twelve crystal scintillators with dimension of $1.5 X_0$.

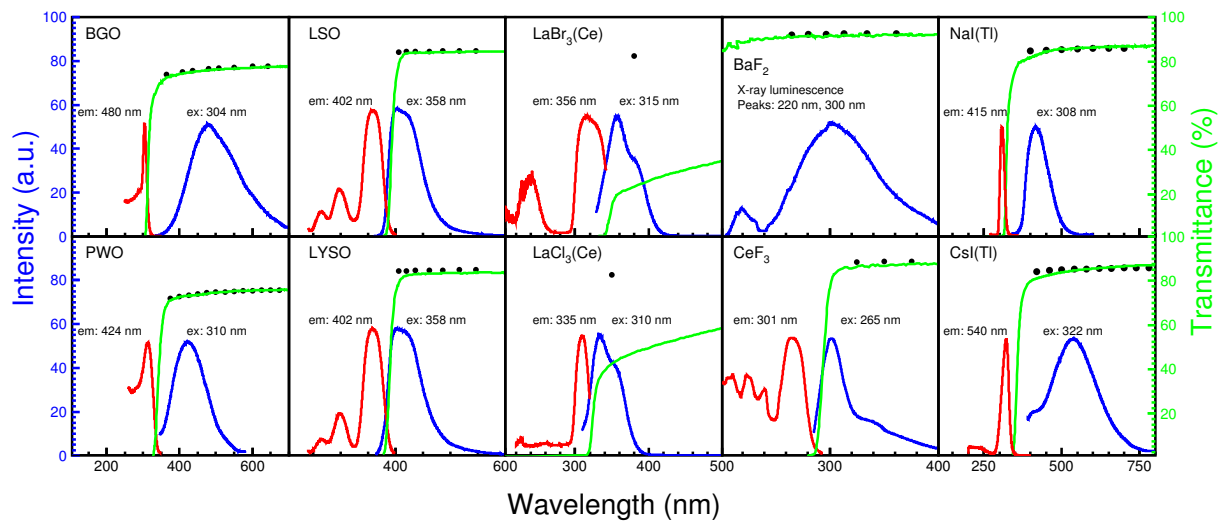


Figure 2. The excitation (red) and emission (blue) spectra (left scale) and the transmittance (green) spectra (right scale) are shown as a function of wavelength for ten crystal scintillators. The solid black dots are the theoretical limit of the transmittance.

and LaCl_3 which are a cylinder with a length of $1.5 X_0$ and areas at two ends equaling to $1.5 \times 1.5 X_0^2$ to match the 2 inch diameter of the PMT cathode.

Figure 2 shows a comparison of the transmittance, emission and excitation spectra as a function of wavelength for ten samples. The solid black dots in these plots are the theoretical limit of the transmittance, which was calculated by using corresponding refractive index as a function of wavelength taking into account multiple bounces between the two parallel end surfaces and assuming no internal absorption [11]. Most samples, except LaBr_3 and LaCl_3 , have their transmittance approaching the theoretical limits, indicating a negligible internal absorption. The poor transmittance measured for LaBr_3 and LaCl_3 samples is probably due to scattering centers inside these samples.

It is interesting to note that BaF_2 , BGO, NaI(Tl) , CsI(Tl) and PbWO_4 have their emission

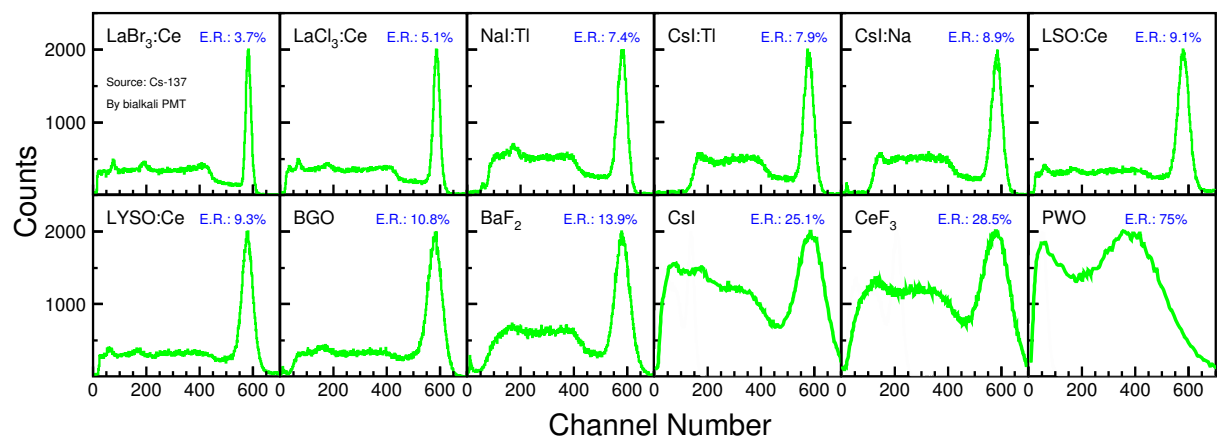


Figure 3. ^{137}Cs γ -ray pulse height spectra measured by a Hamamatsu R1306 PMT are shown for twelve crystal samples. The numerical values of the FWHM resolution (E.R.) are also shown in the figure.

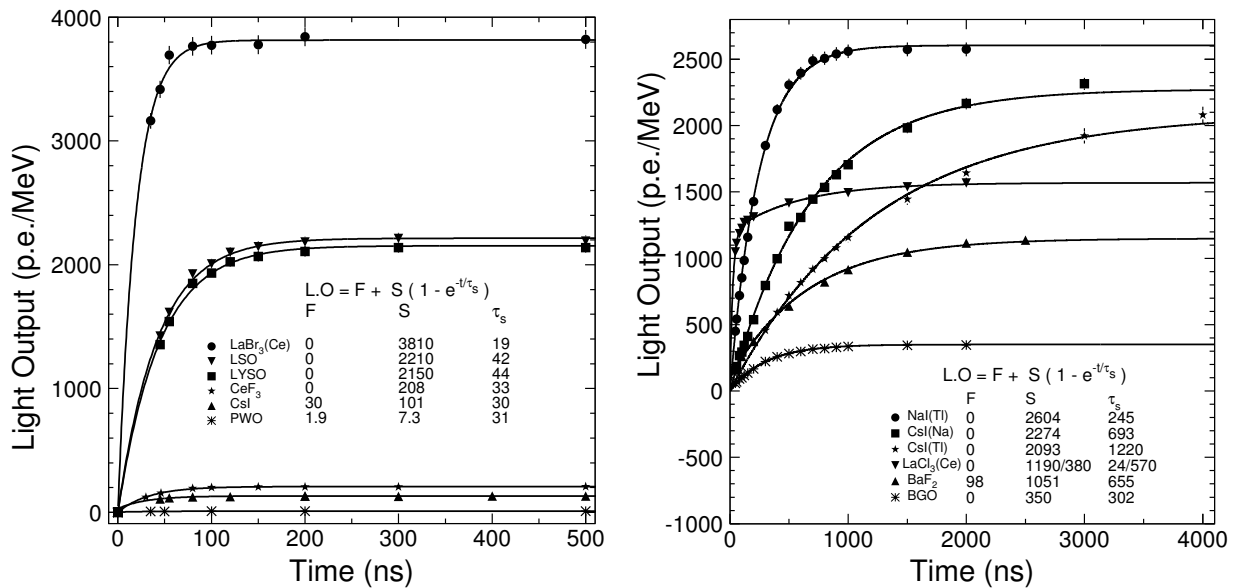


Figure 4. Light output measured by using a XP2254b PMT is shown as a function of integration time for six fast (Left) and six slow (Right) crystal scintillators.

spectra well within the transparent region showing no obvious self-absorption effect. The UV absorption edge in the transmittance spectra of LSO, LYSO, CeF₃, LaBr₃ and LaCl₃, however, cuts into the emission spectra and thus affects crystal's light output. This self-absorption effect is more serious in long crystal samples used in high energy and nuclear physics experiment as discussed for LSO and LYSO crystals [12]. It is well known that a good light response uniformity is crucial to maintain a small constant term for a crystal calorimeter.

Figure 3 shows the ¹³⁷Cs γ -ray pulse height spectra measured by a Hamamatsu R1306 PMT with bi-alkali cathode for twelve crystal samples. Also shown in these figures are the corresponding FWHM energy resolution (E.R.). γ -rays spectroscopy with a few percents resolution is required to identify isotopes for the homeland security application. It is clear that only LaBr₃ approaches this requirement. All other crystals do not provide sufficient energy resolution at low energies.

Figure 4 shows light output in photo-electrons per MeV energy deposition as a function of the integration time, measured by using a Photonis XP2254b PMT with multi-alkali photo cathode, for six fast crystal scintillators (Left): LaBr₃, LSO, LYSO, CeF₃, undoped CsI and PbWO₄ and six slow crystal scintillators (Right): NaI(Tl), CsI(Na), CsI(Tl), LaCl₃, BaF₂ and BGO. The corresponding fits to the exponentials and their numerical results are also shown in these

Table 2. Emission Weighted Quantum Efficiencies (%)

Emission	LSO/LYSO	BGO	CsI(Tl)
Hamamatsu R1306 PMT	12.9±0.6	8.0±0.4	5.0±0.3
Hamamatsu R2059 PMT	13.6±0.7	8.0±0.4	5.0±0.3
Photonis XP2254b	7.2±0.4	4.7±0.2	3.5±0.2
Hamamatsu S2744 PD	59±4	75±4	80±4
Hamamatsu S8664 APD	75±4	82±4	84±4

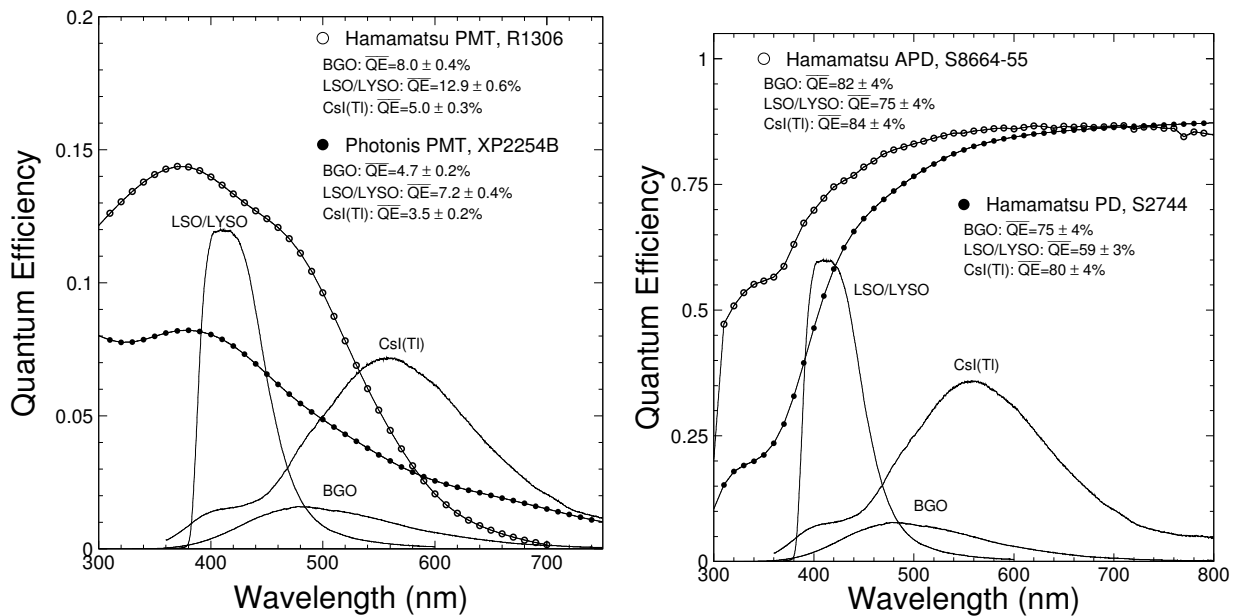


Figure 5. Left: Quantum efficiencies of a Hamamatsu 1306 PMT with bi-alkali cathode (open circles) and a Photonis 2254B PMT with multi-alkali cathode (solid dots) are shown as a function of wavelength together with the emission spectra of the LSO/LYSO, BGO and CsI(Tl) samples, where the area under the emission curves is proportional to their corresponding absolute light output. Right: The same for a Hamamatsu S8664 Si APD (open circles) and a Hamamatsu S2744 Si PIN diode (solid dots).

figures. The undoped CsI, PbWO_4 , LaCl_3 and BaF_2 crystals are observed to have two decay components. Despite its poor transmittance the cerium doped LaBr_3 is noticed by its bright fast scintillation, leading to the excellent energy resolution for the γ -ray spectroscopic applications. The LSO and LYSO samples have consistent fast decay time (~ 40 ns) and photo-electron yield, which is 6 and 230 times of BGO and PbWO_4 respectively.

Since the quantum efficiency of the PMT used for the light output measurement is a

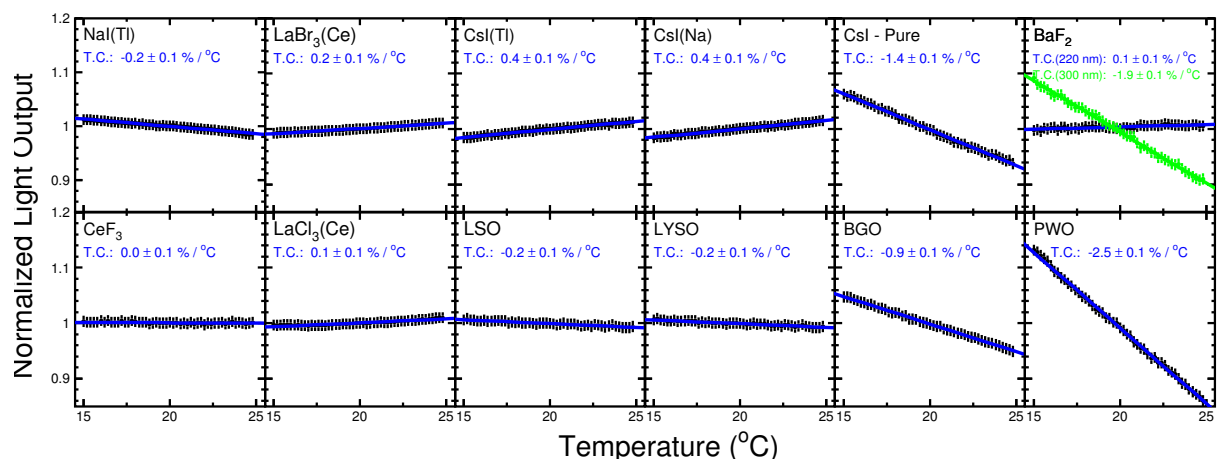


Figure 6. Light output temperature coefficient obtained from linear fits between 15°C and 25°C for twelve crystal scintillators.

function of wavelength, it should be taken out to directly compare crystal's light output. Figure 5 shows typical quantum efficiency as a function of wavelength for a PMT with bi-alkali cathode (Hamamatsu R1306) and a PMT with multi-alkali cathode (Photonis 2254B), a Si APD (Hamamatsu S8664) and a Si PIN PD (Hamamatsu S2744). The emission spectra of LSO/LYSO, BGO and CsI(Tl) crystals are also shown in these figures. Table 2 summarized numerical result of the emission weighted average quantum efficiency for several readout devices. The light output values in Table 1 are listed with the PMT quantum efficiency taken out. The light output of LSO and LYSO crystals is a factor of 4 and 200 of that of BGO and PbWO_4 respectively.

Scintillation light yield from crystal scintillators may also depends on the temperature. Fig 6 shows light output variations for twelve crystal samples between 15°C and 25°C . The corresponding temperature coefficients obtained from linear fits are also listed in the figure. The numerical result of these fits is also listed in Table 1.

3. LSO/LYSO Crystal Calorimeter

Large size LSO and LYSO crystals are routinely grown in industry [12]. Figure 7 shows four long crystal samples of $2.5 \times 2.5 \times 20 \text{ cm}^3$ from CTI Molecular Imaging (CTI), Crystal Photonics, Inc. (CPI), Saint-Gobain Ceramics & Plastics, Inc. (Saint-Gobain) and Sichuan Institute of Piezoelectric and Acousto-optic Technology (SIPAT). Figure 8 shows the spectra of 0.51 MeV γ -rays from a ^{22}Na source observed with coincidence triggers [12]. The readout devices used are a Hamamatsu R1306 PMT (Left) and two Hamamatsu S8664-55 APDs (Right). The FWHM resolution for the 0.51 MeV γ -ray is about 12% for the PMT readout, which can be compared to 15% for the BGO sample. With the APD readout, the γ -ray peaks are clearly visible. The energy equivalent readout noise was less than 40 keV for these long LSO and LYSO samples.

LSO/LYSO crystals is also found to be much more radiation hard than other crystals commonly used in high energy and nuclear physics experiment, such as BGO, CsI(Tl) and PbWO_4 [13]. Their scintillation mechanism is not damaged by γ -ray irradiation. Radiation damage in LSO and LYSO crystals recovers very slow under room temperature but can be completely cured by thermal annealing at 300°C for ten hours. The energy equivalent γ -ray induced readout noise was estimated to be about 0.2 MeV and 1 MeV respectively in a

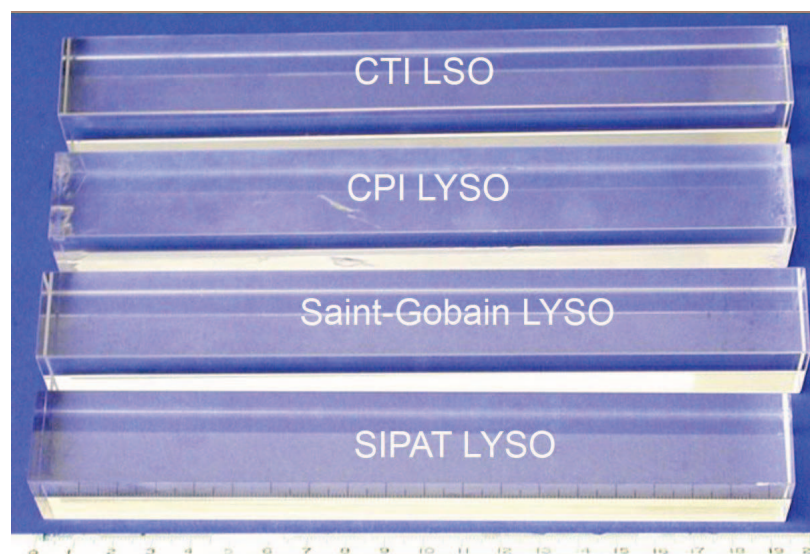


Figure 7. A photo shows four long crystal samples with dimension of $2.5 \times 2.5 \times 20 \text{ cm}^3$.

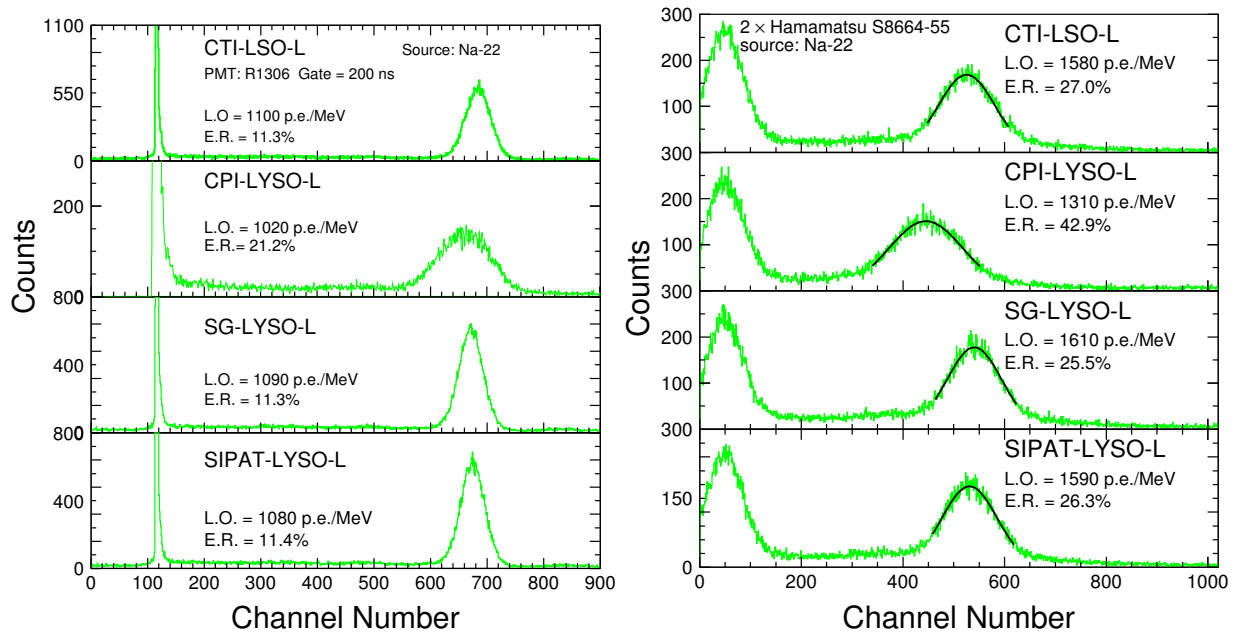


Figure 8. The spectra of 0.511 MeV γ -rays from a ^{22}Na source, measured by a Hamamatsu R1306 PMT (Left) and two Hamamatsu S8664-55 APDs (Right), with a coincidence trigger for four long LSO and LYSO samples from CTI, CPI, Saint-Gobain and SIPAT.

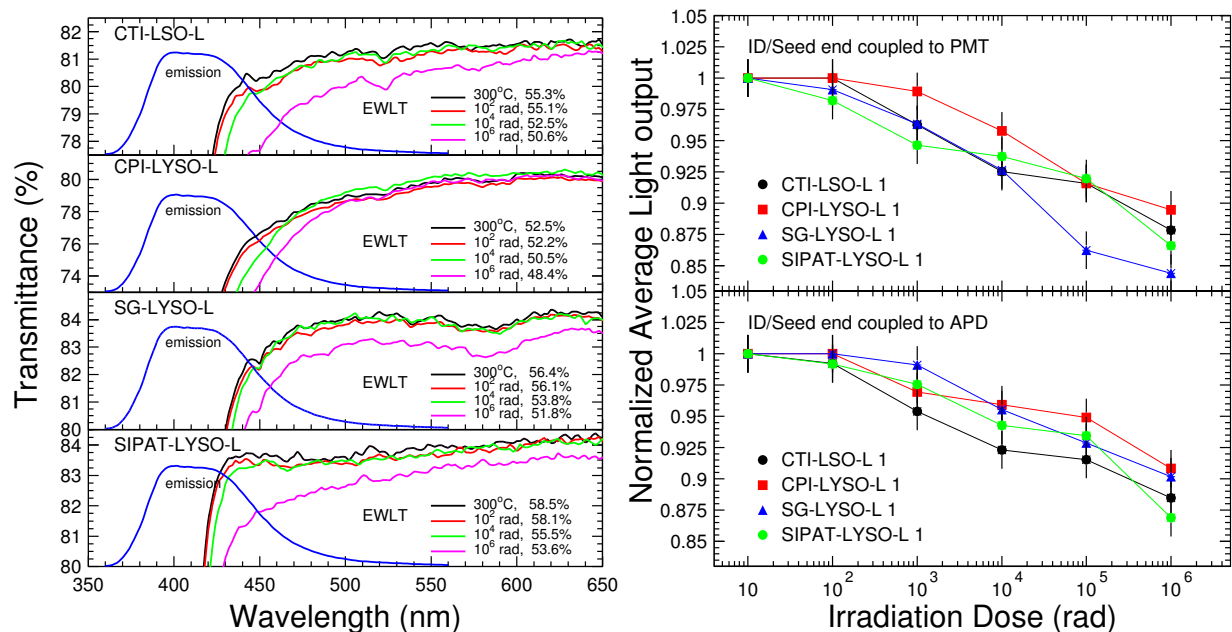


Figure 9. Left: The longitudinal transmittance spectra are shown as a function of wavelength in an expanded scale together with the photo-luminescence spectra for four LSO and LYSO samples before and after the irradiation with integrated doses of 10^2 , 10^4 and 10^6 rad. Right: The normalized light output is shown as a function of the integration dose for four long LSO and LYSO samples with PMT (top) and APD (bottom) as the readout devices.

radiation environment of 15 rad/h and 500 rad/h for LSO and LYSO samples of $2.5 \times 2.5 \times 20$ cm³ [7]. Figure 9 (Left) shows an expanded view of the longitudinal transmittance spectra for three samples before and after several steps of the γ -ray irradiation with integrated dose of 10^2 , 10^4 and 10^6 rad. Also shown in the figure is the corresponding numerical values of the photo-luminescence weighted longitudinal transmittance (*EWLT*). Figure 9 (Right) shows the normalized average light output as a function of integrated dose for five long samples from various vendors. It is interesting to note that all samples show consistent radiation resistance with degradations of both the light output and transmittance at 10 to 15% level after γ -ray irradiation with an integrated dose of 1 Mrad.

4. Summary

In a brief summary, LSO/LYSO crystals are an excellent material for a total absorption electromagnetic calorimeter for a future high-energy physics experiment in a severe radiation environment. Assuming the same APD-based readout scheme used for the CMS PWO calorimeter, the expected energy resolution of a LSO/LYSO crystal based electromagnetic calorimeter would be

$$\sigma_E/E = 2\%/\sqrt{E} \oplus 0.5\% \oplus 0.001/E, \quad (1)$$

where the stochastic term is dominated intrinsically by the fluctuation of shower leakage as indicated by GEANT simulations. This represents a fast calorimeter over a large dynamic range with very low noise. Thanks also to the LSO/LYSO low temperature coefficient, such a calorimeter is less demanding to the experimental environment. Because of the crystals excellent radiation hardness, a LSO/LYSO crystal calorimeter is capable of making precision measurement for electrons, photons and jets and thus provides a great physics discovery potential in a severe radiation environment, like the HL-LHC.

Acknowledgments

This work is partially supported by the U.S. Department of Energy Grant No. DE-FG03-92-ER40701 and the U.S. National Science Foundation Award PHY-0612805 and PHY-0516857.

References

- [1] C. Melcher and J. Schweitzer, *Cerium-doped lutetium oxyorthosilicate: a fast, efficient new scintillator*, *IEEE Trans. Nucl. Sci.* **39** (1992) 502–505.
- [2] D.W. Cooke, K.J. McClellan, B.L. Bennett, J.M. Roper, M.T. Whittaker and R.E. Muenchausen, *Crystal growth and optical characterization of cerium-doped $Lu_{1.8}Y_{0.2}SiO_5$* , *J. Appl. Phys.* **88** (2000) 7360–7362.
- [3] T. Kimble, M Chou and B.H.T. Chai, *Scintillation properties of LYSO crystals*, in *Proc. IEEE Nuclear Science Symposium Conference* (2002).
- [4] C. Cecchi, “A LYSO Calorimeter for a SuperB Factory ,” in these Proceedings.
- [5] F. Happacher , *CCALT: Crystal Calorimeter at KLOE2*, in these Proceedings.
- [6] The Mu2e Experiment, see <http://mu2e.fnal.gov/>.
- [7] R.H. Mao, L.Y. Zhang and R.-Y. Zhu, *Gamma Ray Induced Radiation Damage in PWO and LSO/LYSO Crystals*, Paper N32-5 in NSS 2009 Conference Record (2009).
- [8] R.H. Mao, L.Y. Zhang and R.-Y. Zhu, *Effect of Neutron Irradiations in Various Crystal Samples of Large Size for Future Crystal Calorimeter*, Paper N32-4 in NSS 2009 Conference Record (2009).
- [9] F. Nessi-Tedaldi, G. Dissertori, P. Lecomte, D. Luckey and F. Pauss, *Studies of Cerium Fluoride, LYSO and Lead Tungstate Crystals Exposed to High Hadron Fluences*, Paper N32-3 in NSS 2009 Conference Record (2009).
- [10] R.H. Mao, L.Y. Zhang and R.-Y. Zhu, *Optical and Scintillation Properties of Inorganic Scintillators in High Energy Physics*, *IEEE Trans. Nucl. Sci.* **NS-55** (2008) 2425–2431.
- [11] D.A. Ma and R.-Y. Zhu, *Nucl. Instr. and Meth.* **A333** (1993) 422.
- [12] J.M. Chen, R.H. Mao, L.Y. Zhang and R.-Y. Zhu, *IEEE Trans. Nucl. Sci.* **54** (2007) 718.
- [13] J.M. Chen, R.H. Mao, L.Y. Zhang and R.-Y. Zhu, *IEEE Trans. Nucl. Sci.* **54** (2007) 1319.